CHAPTER 4

Well Tie and Wavelet Extraction Results

Well ties and wavelet extractions were carried out using the Jason Workbench software. There are five main panels which were integrated to associate well tying, as shown in Figure 4-1. Seismic and synthetics traces were displayed on the first two panels as wiggle displays, respectively, with the well path in overlay. Third panel was displayed correlation coefficient which calculated along well path within the selected window. Stretch and squeezing or bulk shifting a synthetic trace in time panel are actually modifying time-depth relationship, which shown on drift curve. Drift curve was expressed between differentiated of time-depth (slowness) and the sonic log, as shown in the fourth panel. The slowness in microsecond per feet in last panel was used to compare the measured sonic log and recent differentiated time-depth relationship (Δt).

The input seismic dataset used in this study was processed to ensure the wavelet being zero phases with reverse polarity following the SEG standard. An increase in acoustic impedance will be represented by a trough in the seismic dataset, according to this definition. The polarity was confirmed by the wavelet of the seabed reflector due to it was generated from positive reflectivity; seismic wave travelling from low acoustic impedance (sea water) to higher acoustic impedance layer (seabed). When red is negative amplitude and seabed reflector is red. So, polarity is SEG standard (Figure 4-2).

Synthetic traces were computed for Wells-A, -C and -D to achieve time-depth relationships for each of these three wells. At each well location, wavelets were extracted for near, mid and far angle stacks within a 1000 to 2400 ms window, and the wavelet length was 100 ms (Figure 4-3). The wavelets for Well-A did not follow the same trend as the ones extracted at Well-C and Well-D, which both aligned in phase and amplitude. The wavelets extracted from Well-A was excluded when constructing a final

multi-wells (average) wavelet. The final average wavelets were computed using Wells-C and -D wavelets, as shown in Figure 4-4. It should also be noted that the available log data for Well-B was limited to within 300 ms of seismic section, and did not provide enough data to ensure a stable wavelet extraction. Well-B was therefore not considered to be part of the wavelet extraction.

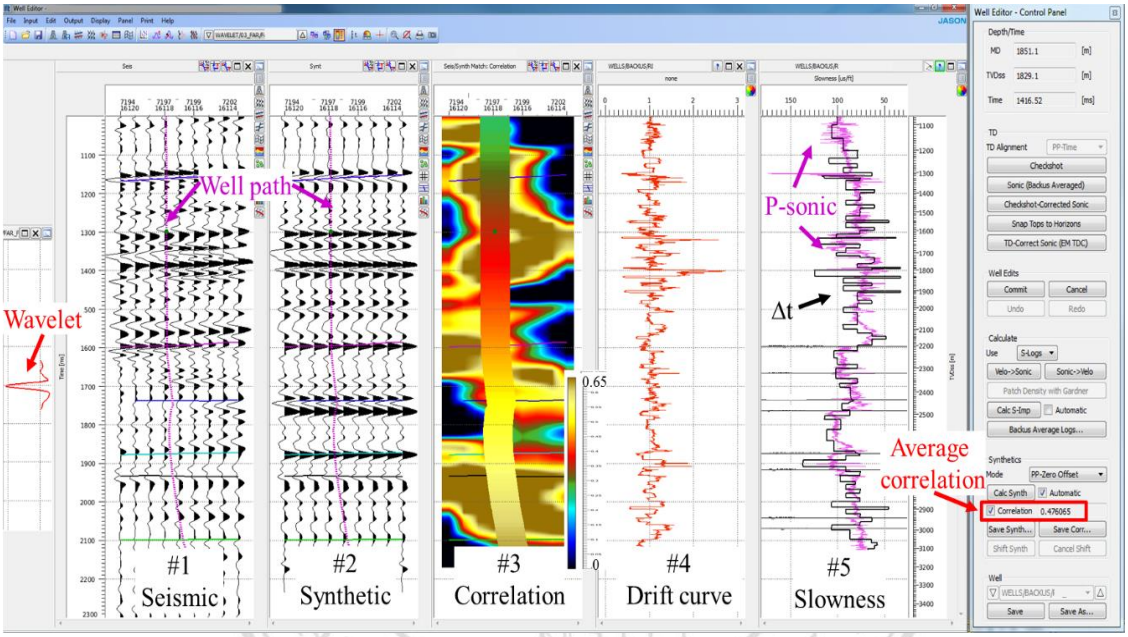

Figure 4-1 Well Editor module of Jason Workbench software using for well tie.

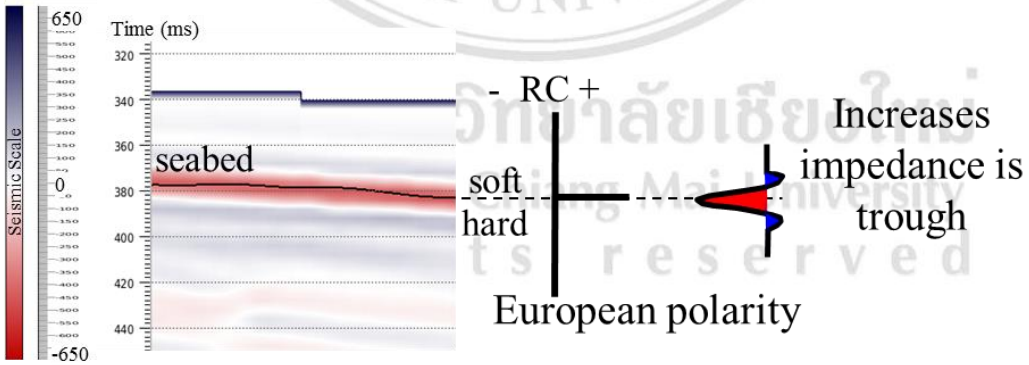

Figure 4-2 Wavelet polarity convention of the seismic input data used in this study.

The final well ties were carried out by using the average wavelets for near, mid and far angle stacks. The final well ties for mid angle stack of Wells-A, -C and -D can be observed in Figures 4-4, 4-5 and 4-6, respectively (the final well ties for near and far

angle stack were shown in APPENDIX B). The final well ties provided the final time and depth relations for the seismic dataset at the respective input well locations. Figure 4-7 were shown the well locations and the arbitrary line which used to compare synthetic traces of each wells for near, mid and far angle stack in the Figures 4-8, 4-9 and 4-10, respectively. The overall well tie was best at Well-C, while being considered to be moderate to good at both Wells-A and -D. A summary of the well ties using both the extracted and average wavelets can be observed in Table 4-1.

Table 4-1 Summary of the correlation coefficients when performing the well tie at each wells using the respective final time-depth relationships

CORRELATION COEFFICIENT				
SEISMIC ANGLE STACK	WAVELET	WELL		
		A	C	D
NEAR	Extracted	0.335	0.484	0.380
	Average	0.304	0.450	0.424
MID	Extracted	0.424	0.447	0.430
	Averaged	0.338	0.441	0.412
FAR	Extracted	0.415	0.354	0.340
	Averaged	0.242	0.356	0.297

The dominant frequency was derived from the amplitude spectrum of the final average wavelet from the mid angle stack. The result was used to estimate the vertical seismic resolution, following the calculation below:

Maximum frequency (f) = 45 Hz,

Average velocity (within sandstone) measured from well log data; v = 4025 m/s,

Wavelength; $\lambda = \frac{v}{f}$,

$\lambda = 4025/45$,

$\lambda = 89.4$ m.

Tuning thickness (vertical resolution); $\lambda/4 = 22.4$ m.

The vertical seismic resolution in seismic data can be estimated, based on the equations seen above, and represents the minimum bed thickness in a layer to ensure separate reflections for “top” and “base”. Based on visual comparison of the lithology log and the lithology cube at well locations considered in this project, a reasonable seismic detectability of sand layers in this area approximately 23 meters. However, the layers observed in seismic data were mainly depended on the acoustic impedance contrast and the signal-to-noise ratio in the dataset. This is referred to as “seismic detectability”. As a general rule of thumb a low impedance hydrocarbon filled sand with reasonable seismic data quality have a seismic detectability of λ/20 to λ/30, which in this case would be 3 – 4.5 m. However, as the acoustic impedance contrast between shale and sand is very small at the target considered in this study, it is expected that the detectability is much lower.

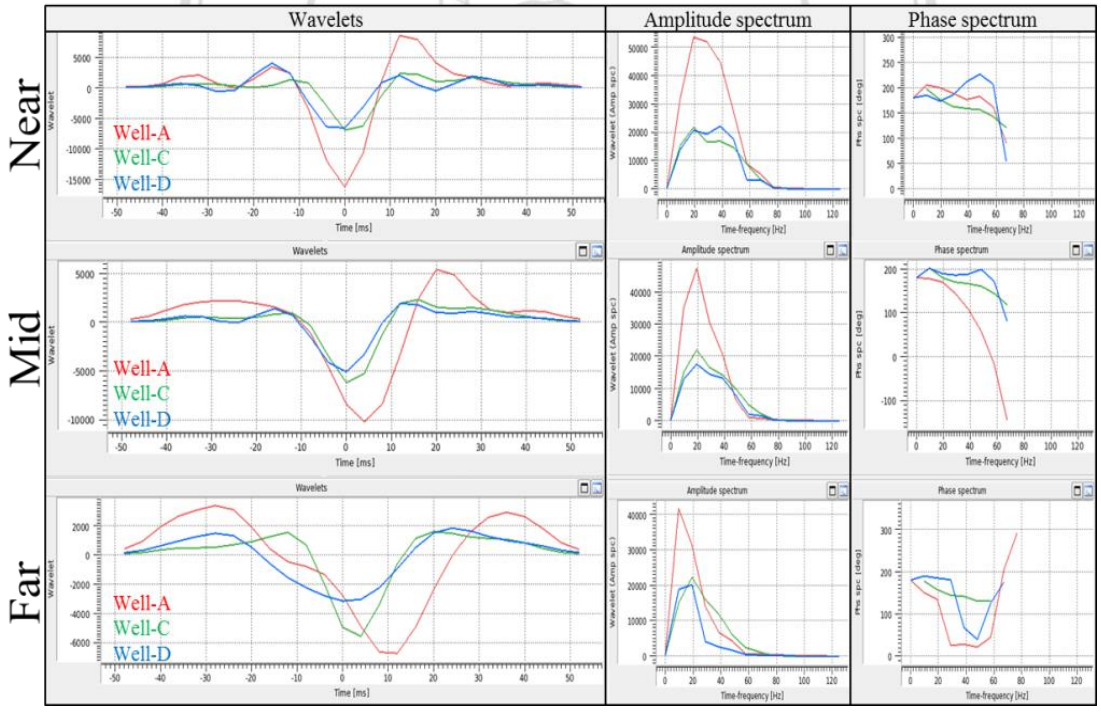

Figure 4-3 Extracted wavelets at well locations Wells-A, -C and -D for all angle stacks.

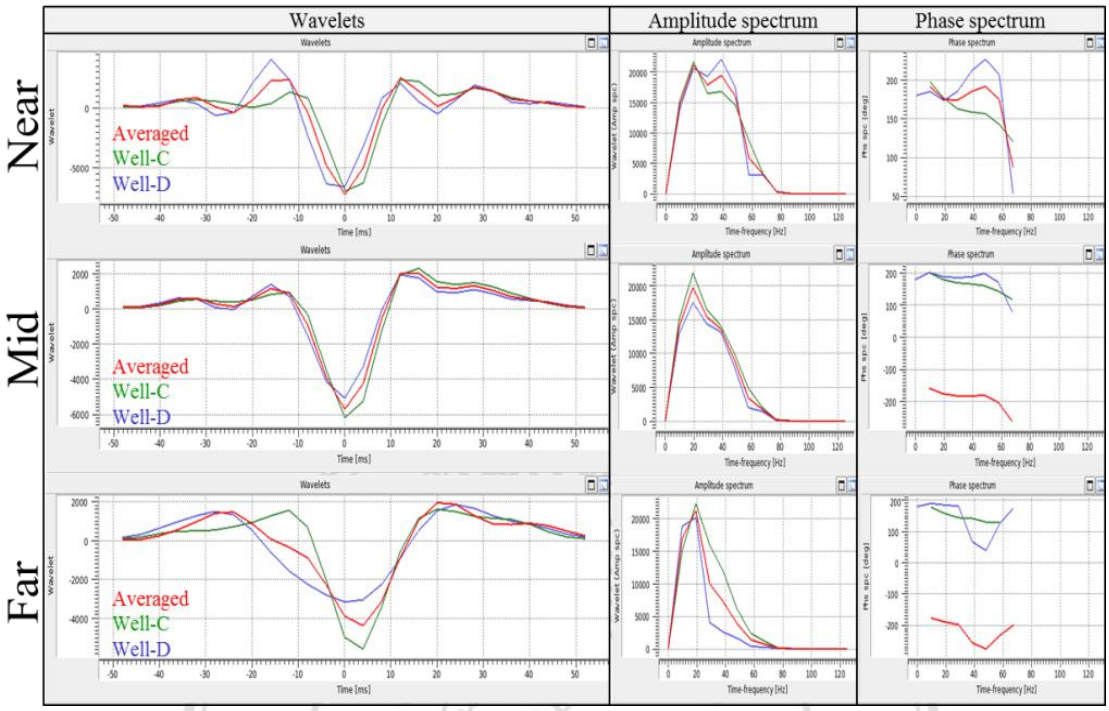

Figure 4-4 Final average wavelets, extracted using only Well-C and Well-D for all angle stacks.

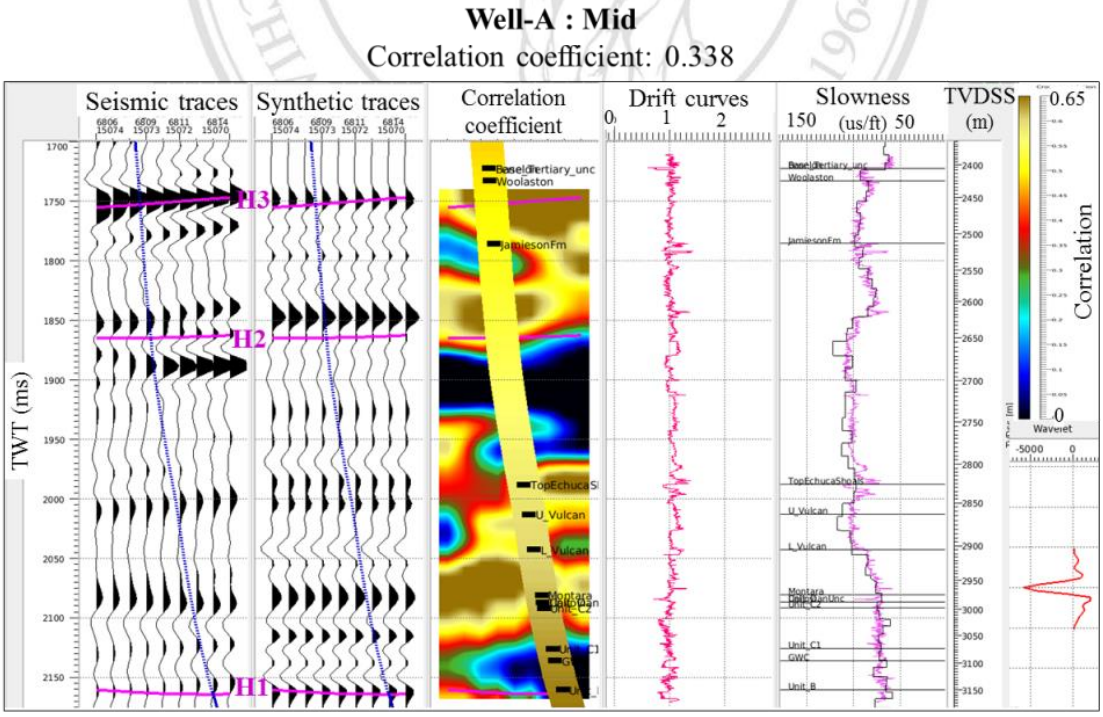

Figure 4-5 Synthetic tie at Well-A showing the tie at mid angle stack.

Well-C : Mid

Correlation coefficient: 0.441

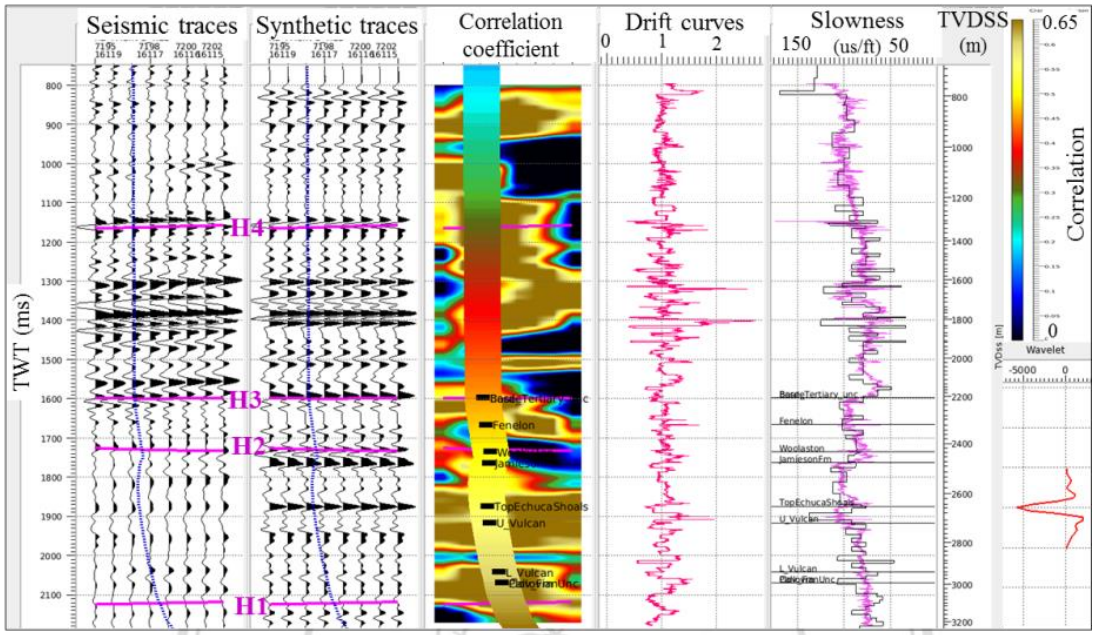

Figure 4-6 Synthetic tie at Well-C showing the tie at mid angle stack

Well-D : Mid

Correlation coefficient: 0.412

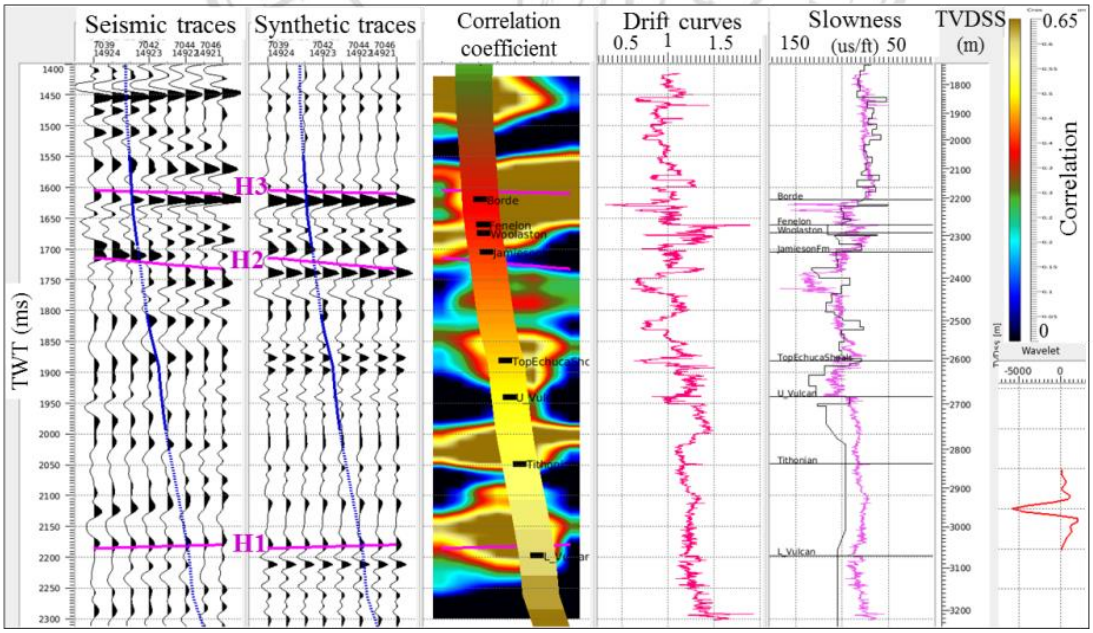

Figure 4-7 Synthetic tie at Well-D showing the tie at mid angle stack.

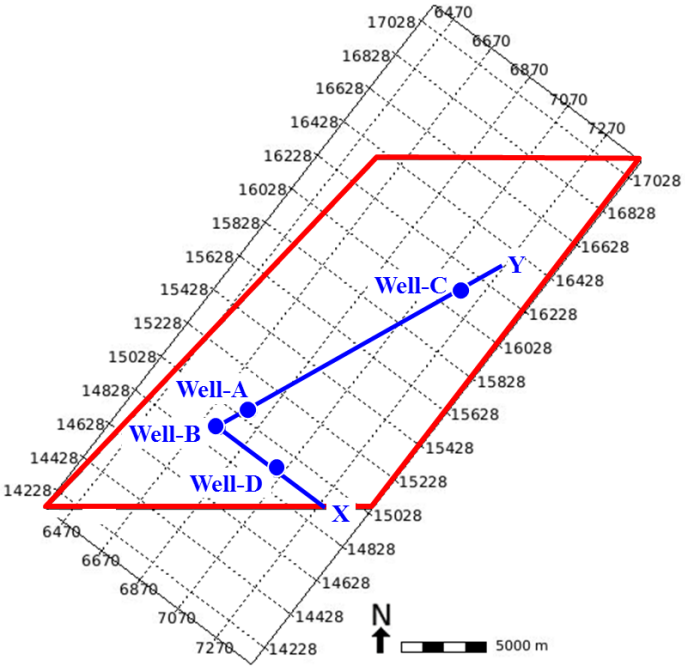

Figure 4-8 Well locations and the arbitary line was used to show the well tie result.

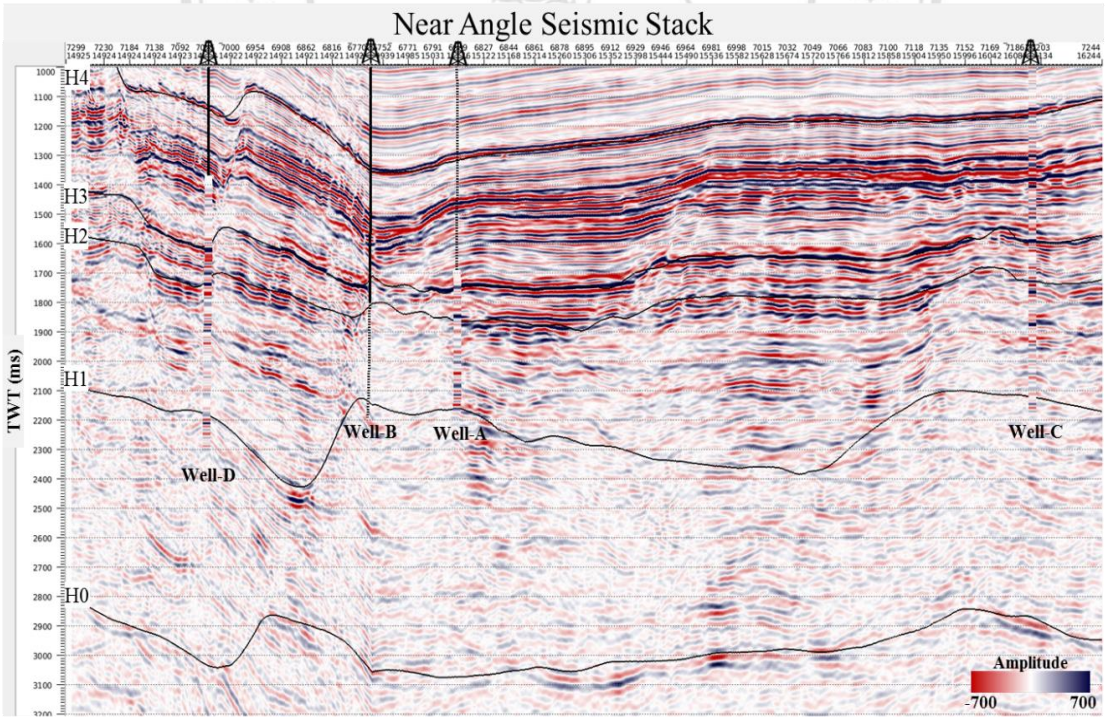

Figure 4-9 The arbitrary line of near angle stack was overlaid by Wells-A, -C and -D synthetic traces.

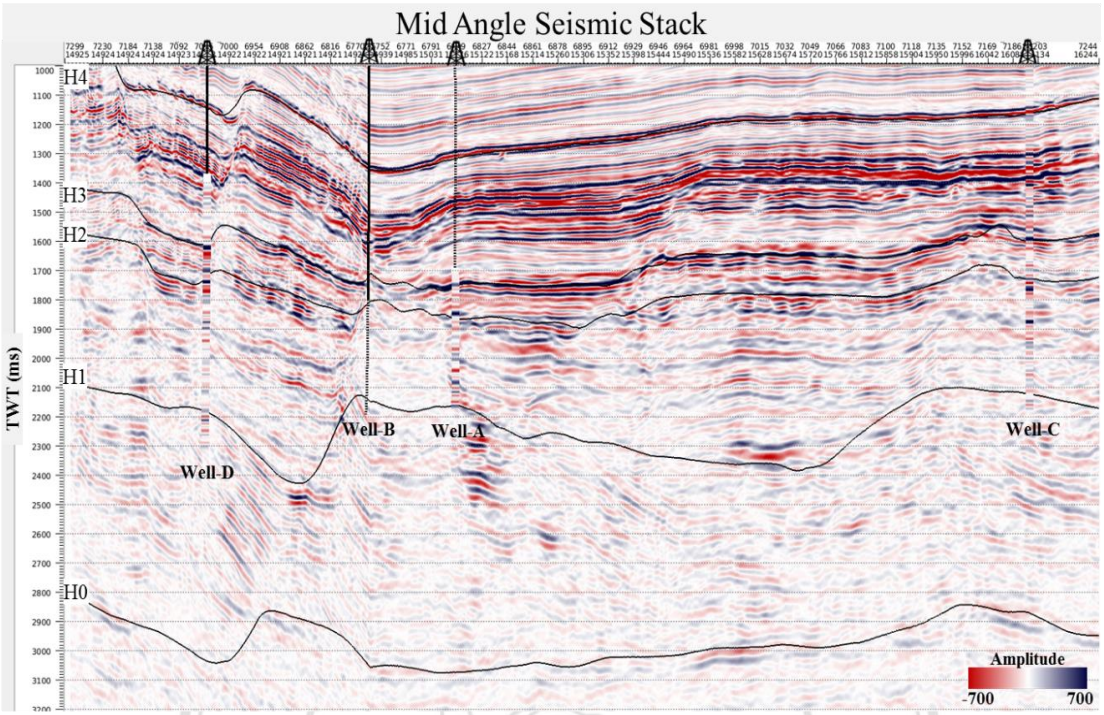

Figure 4-10 The arbitrary line of mid angle stack was overlaid by Wells-A, -C and -D synthetic traces.

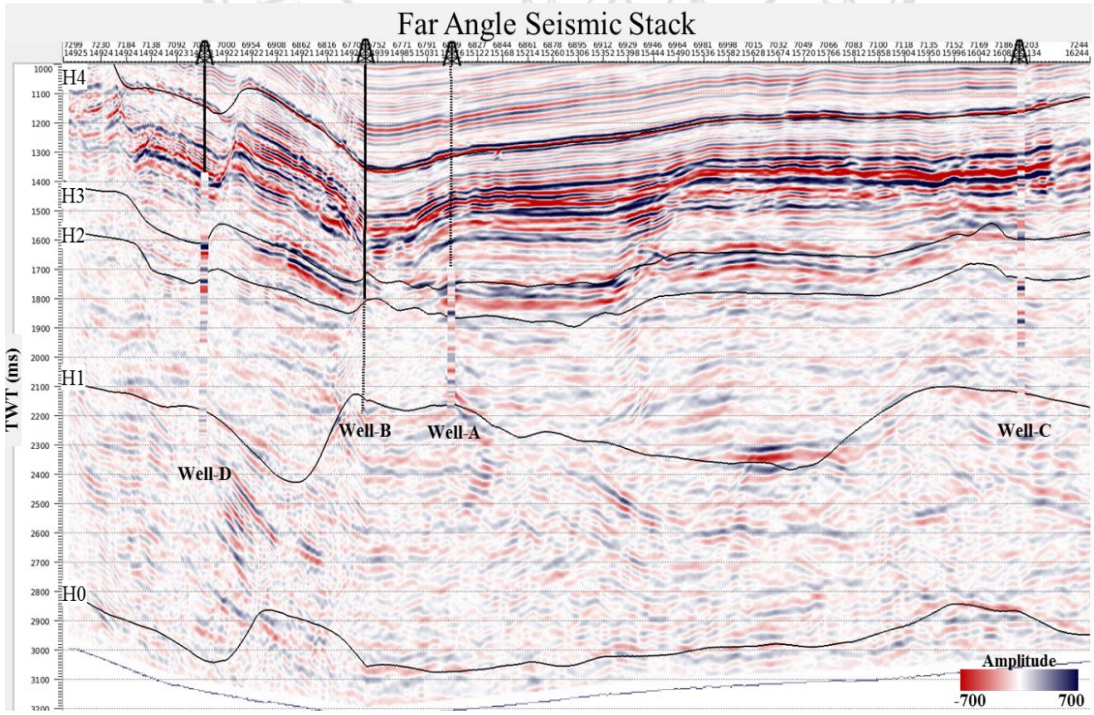

Figure 4-11 The arbitrary line of far angle stack was overlaid by Wells-A, -C and -D synthetic traces.